Supplementary Information

Waste eliminated by waste: Industrial o-phenylenediamine residue derived N,O co-doped hierarchical porous carbon for efficient o-nitroaniline removal

Zheng Lei[a], Dong-Sheng Li[a], Guang-Wen Xu[a*], Yu-Guo Li[b], Yu-Ling Shan[a], Jun-Wei Ding[a*], Wen-Long Yu[a*]

[a] *State Key Laboratory Base of Eco-chemical Engineering, College of Chemical Engineering, Qingdao University of Science and Technology, Qingdao, 266042, China*

[b] *Qingdao No.58 High School of Shandong Province, Qingdao, 266041, China*

**Corresponding author. Guang-Wen Xu E-mail addresses: xugw@qust.edu.cn*

**Corresponding author. Jun-Wei Ding E-mail addresses: djwnsfc@126.com*

**Corresponding author. Wen-Long Yu E-mail addresses: yuwl@qust.edu.cn*

1. Adsorption experiment

The batch process of ONA removal was performed in the 100 mL container with ONA (500 mg·L^{-1}). The adsorption experiment was undertaken in a constant temperature oscillation chamber with a rotational speed of 150 rpm, then 20 mg AWCs were put into the container to start the adsorption for 12 h. Before mixing, AWCs were dried under vacuum at 200 °C for 2 h, and the pH of ONA solution was not adjusted. Subsequently, the mixed solution was subjected to solid-liquid separation using a filter membrane (0.45 μm), and the concentration of ONA in the aqueous solution was determined by an ultraviolet-visible spectrophotometer at 238 nm. The experiment was repeated three times, and the results were averaged. The calculation formula of equilibrium adsorption capacity is:

$$q_e = \frac{(C_0 - C_e)}{m} \times V \# S1$$

Among them, C_0 is the initial concentration of ONA (mg·L^{-1}), Ce is the equilibrium concentration of ONA (mg·L^{-1}), m is the addition amount of AWCs (g), V is the volume of ONA aqueous solution (mL), and qe is the equilibrium adsorption capacity of ONA (mg·g^{-1}).

2. Adsorption isotherms test

By measuring the adsorption isotherms, the relationship between the adsorbate concentration and the adsorption capacity was accurately expressed and the adsorption behavior of ONA on AWC-M-1 and AWC-K-1 was explored. Before the start of the experiment, 30-300 mg·L^{-1} ONA aqueous solution was prepared, and AWC-M-1 and AWC-K-1 were vacuum treated at 200 °C for 2 hours. 0.02 g of each adsorbent (AWC-

M-1 and AWC-K-1) was mixed with 50 mL different concentrations of ONA aqueous solution, and continuously oscillated for 12 h at 25 °C and 150 rpm with a constant temperature water bath shaker. After adsorption equilibrium, the mixed solution was separated by 0.45 μm filter membrane, and the concentration of ONA in aqueous solution was determined by ultraviolet-visible spectrophotometer at 238 nm. The experiment was repeated three times, and the results were averaged. The Langmuir/Freundlich model was used to fit the experimental data.

Langmuir isotherm model is given in Eq. (S2).

$$q_e = \frac{Q_0 K_L C_e}{1 + K_L C_e} \# S2$$

where Q_0 is the adsorption capacity ($mg \cdot g^{-1}$) and K_L is Langmuir constant ($L \cdot mg^{-1}$).

Freundlich isotherm model is represented in Eq. (S3).

$$q_e = K_F C_e^{\frac{1}{n}} \# S3$$

where K_F(($mg \cdot g^{-1}$)·($L \cdot mg^{-1}$)1·n^{-1}) and n are the Freundlich adsorption constants related to the adsorption capacity and adsorption intensity, respectively.

3. Adsorption kinetics test

ONA aqueous solution (200 $mg \cdot L^{-1}$) was prepared for the adsorption kinetics test. 0.02 g of each adsorbent (AWC-M-1 and AWC-K-1) was separately mixed with 50 mL of ONA aqueous solution, and the mixture was shaken for 1-60 min at 25 °C and 150 rpm with a constant temperature water bath shaker. After that, the mixed solution was separated by 0.45 μm filter membrane, and the concentration of ONA in aqueous solution was determined by ultraviolet-visible spectrophotometer at 238 nm. The experiment was repeated three times, and the results were averaged. The PSO/PFO model was used to fit the experimental data.

PSO and PFO kinetics models are represented in Eq. (S4) and (S5).

$$Q_t = Q_{e1}\left(1 - e^{-k_1 t}\right) \#S4$$

$$Q_t = \frac{k_2 Q_{e2}^2 t}{\left(1 + k_2 Q_{e2} t\right)} \#S5$$

where Q_t is the ONP adsorption capacity at required time t, and the equilibrium adsorption capacity Q_{e1} and Q_{e2} ($mg \cdot g^{-1}$) can be determined by PFO and PSO models. k_1 (min^{-1}), k_2 ($g \cdot mg^{-1} \cdot min^{-1}$) are the rate constants of PFO and PSO models, respectively.

The determination coefficient (R^2), adjusted determination coefficient (R^2_{adj}), can be calculated by the following Eq. (S6) and (S7):

$$R^2 = 1 - \frac{\sum_{i=1}^{n}\left(y_{exp} - y_{pred}\right)^2}{\sum_{i=1}^{n}\left(y_{exp} - \bar{y}_{exp}\right)^2} \#S6$$

$$R_{adj}^2 = 1 - \left(1 - R^2\right)\frac{(n-1)}{(n-p-1)} \#S7$$

where y_{exp} and y_{pred} are the experimental value and predicted value, respectively. n is the number of experimental values, and p is the number of parameters based on the model.

4. Fixed-bed adsorption test

The fixed-bed column adsorption experiments were equipped with a plunger pump and a stainless-steel column. The diameter of stainless-steel column is 4.6 mm, and the total length is 50 mm. 0.1 g of the adsorbent (AWC-M-1 or AWC-K-1) was packed into the stainless-steel column, resulting in a packed length of 10 mm. The continuous flow rate of ONA solution was set to 3 mL·min^{-1}, and the concentration of ONA was 100 mg·L^{-1}.

Dynamic equilibrium adsorption capacity is expressed by Eq. (S8).

$$q_e = \frac{QC_0}{m}\int_0^{t_s}\left(1-\frac{C_t}{C_0}\right)dt\#S8$$

where C_e is the concentration of ONA in the effluent (mg·L^{-1}); C_0 is the initial ONA concentration in the feeding fluid (mg·L^{-1}); q_e is the maximum amount of ONA that could be adsorbed (mg·g^{-1}) on the adsorbent packed; m is the mass of adsorbent packed (g); V is the throughput volume (L); and Q is the flow rate of pumped feeding fluid (L·min^{-1}).

The Thomas model is widely used to evaluate column performance and predict breakthrough curves. The non-linear form of the Thomas model is expressed by Eq. (S9).

$$\frac{C_t}{C_0} = \frac{1}{1+exp\left(\frac{k_{Th}q_e m}{Q} - k_{Th}C_0 t\right)}\#S9$$

where C_0 (mg·L^{-1}) and C_t (mg·L^{-1}) are the influent and effluent concentrations of ONA, respectively; k_{Th} is the Thomas rate constant (L·mg^{-1}·min^{-1}); q_e is the equilibrium adsorption capacity (mg·g^{-1}); m is the mass of the adsorbent (g); Q is the volumetric flow rate (L·min^{-1}); and t is the flow time (min).

After the adsorption, the adsorbent was regenerated with methanol solution. The flow rate of methanol was 1 mL·min^{-1} and the desorption temperature was 50 °C. The regeneration stopped when the ONA concentration in the methanol effluent was less than 5 % of the initial solution. The regenerated porous carbon was subjected to a fixed bed adsorption test for 5 cycles.

5. Detailed computational methods

The adsorption mechanism of ONA molecule on porous carbon was revealed by density functional theory calculation. Considering the structural complexity and uncertainty of disordered porous carbon materials, an aperiodic graphene cluster model ($C_{54}H_{20}$) consisting of 54 carbon atoms, 20 hydrogen atoms and 18 unbranched aromatic rings was constructed as the initial structural unit of the porous carbon materials.

All density functional theory calculations were performed by B3LYP hybrid functional, using def2-SVP unit to optimize the model structure and calculate the single point energy. In order to reflect the intermolecular weak forces accurately, Grimme's DFT-D3 was used for correction. Besides, SMD aqueous solvent model was introduced to express the real water environment. All calculations were performed by ORCA software.

The adsorption energy between ONA and AWC can be expressed by the following formula:

$$E_{abs} = E_{AWC\&ONA} - E_{AWC} - E_{ONA} \# S10$$

where E_{abs} is the adsorption (interaction) energy, $E_{AWC\&ONA}$ is the total energy of the adsorption composite after geometric optimization, E_{ONA} and E_{AWC} are the energy of isolated ONA molecule and carbon cluster after geometric optimization, respectively.

The electrostatic potential (ESP) of the ONA molecule and various carbon models were analyzed to reveal the effect of heteroatom functionalization on adsorption behavior of ONA. The interaction within the adsorption system was investigated by noncovalent interactions analysis (NCI) implemented with the Multiwfn 3.7(dev) code. ORCA was used to convert .mol files based the geometry optimized calculations to the .gbw files at B3LYP-D3/def2-SVP level, which can be processed by Multiwfn program. The reduced density gradient isosurfaces maps colored on a blue-green-red scale according to values of sign(λ2) ρnging from -0.03 to 0.02 au were rendered by means of Visual Molecular Dynamics (VMD) software based on the files exported by Multiwfn.

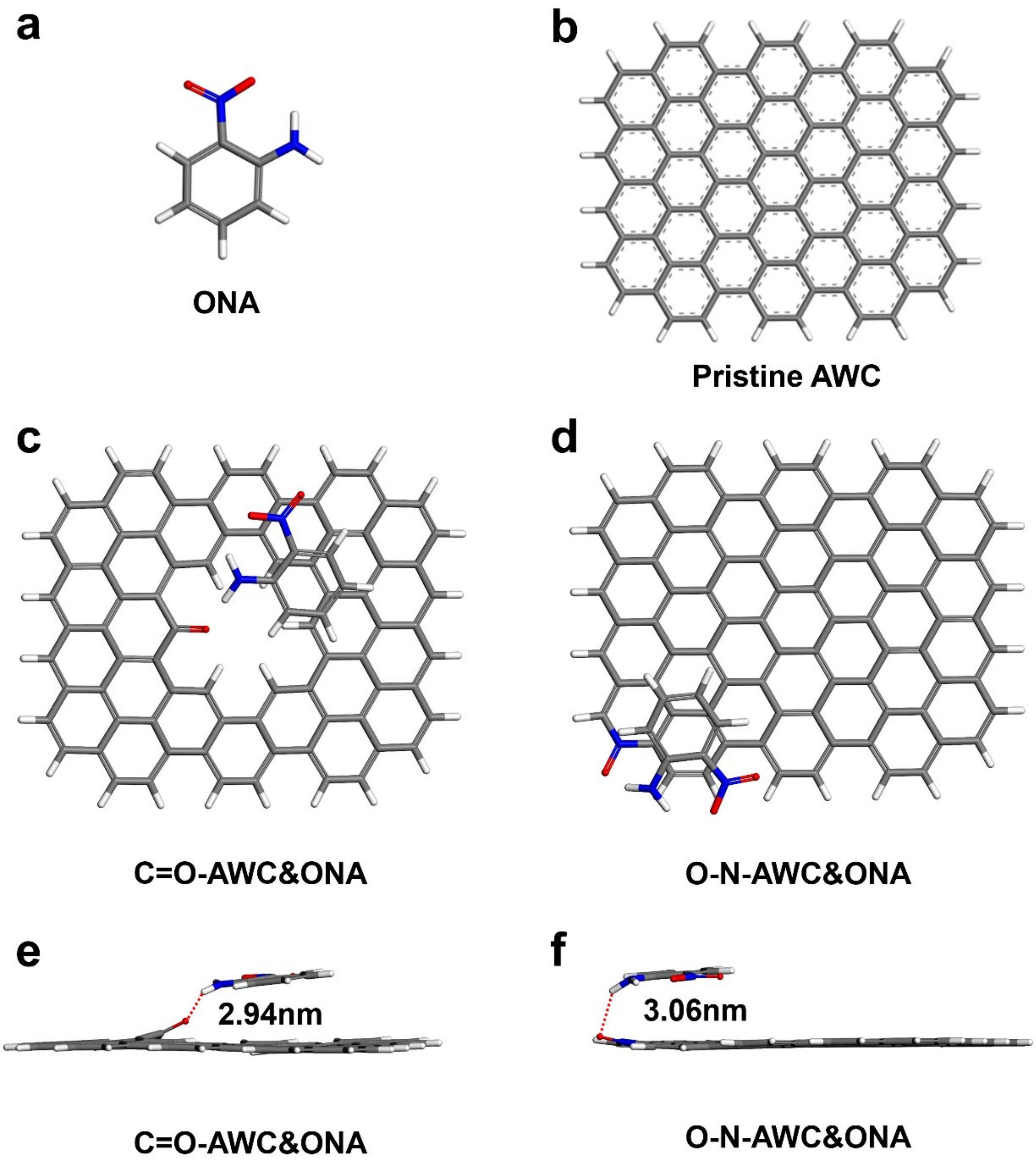

Figure S1. initial configurations of ONA molecular (a); Carbon cluster models (b) and initial models of AWC&ONA (c-f).

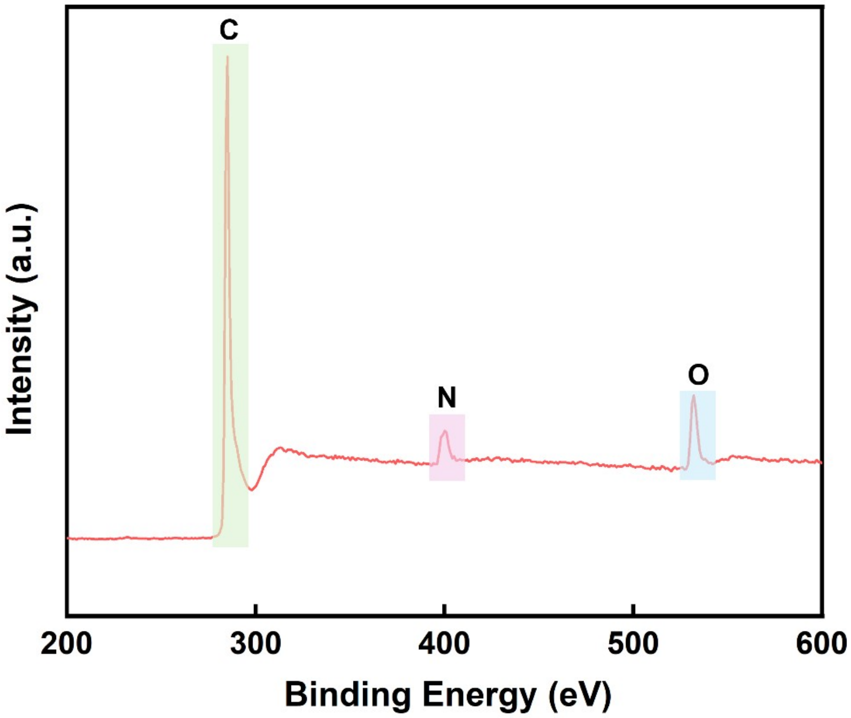

Figure S2. XPS survey spectrum of AWC-M-1.

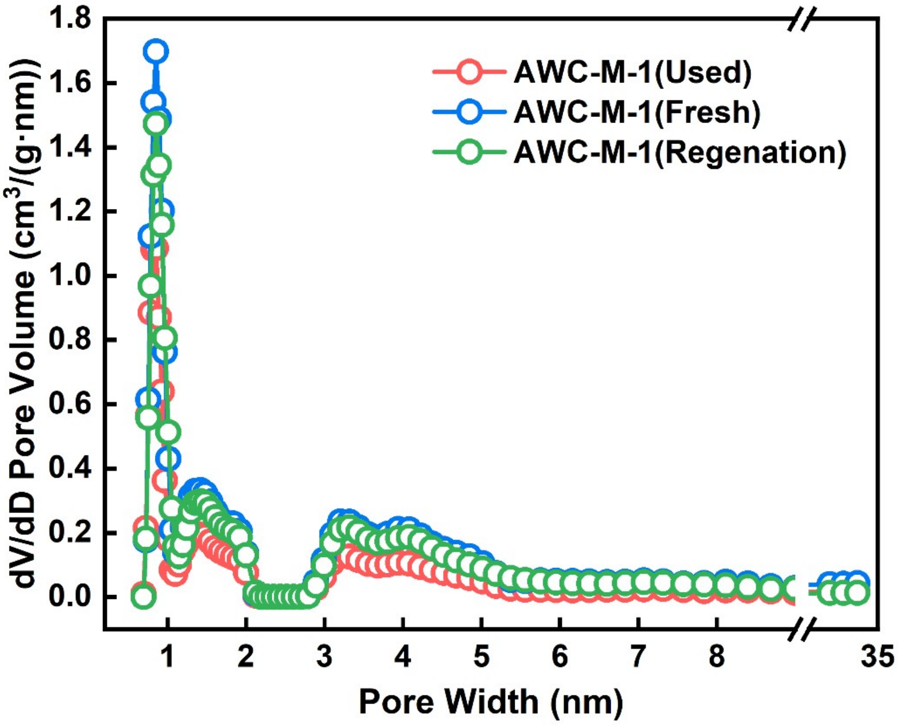

Figure S3. Pore size distribution (0-35 nm) of AWC-M-1 (fresh, used, regeneration) by the NLDFT methods.

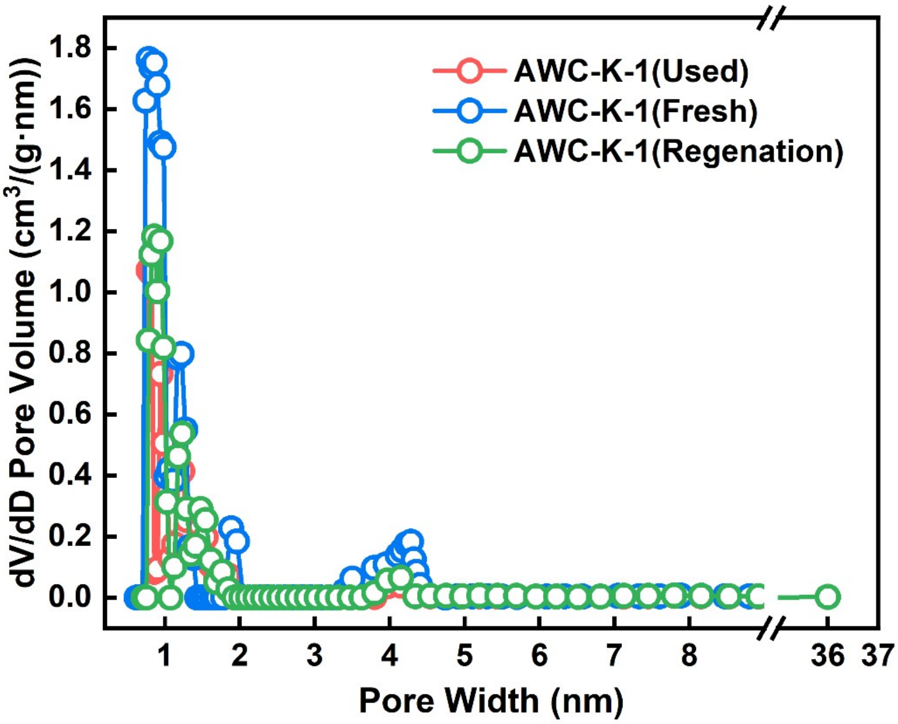

Figure S4. Pore size distribution (0-36 nm) of AWC-K-1 (fresh, used, regeneration) by the NLDFT methods.

Table S1. Chemical Regents.

Chemical Regent	Specification	Manufacturer
$Mg(CH_3COO)_2 \cdot 4H_2O$	AR, 99%	Sinopharm Chemical Reagent Co., Ltd.
CH_3COOH	AR, 99%	Sinopharm Chemical Reagent Co., Ltd.
2-nitroaniline	99.5%	Aladdin Biochemical Technology Co., Ltd.
N_2	99.9%	Yantai DeYi Gas Co., Ltd.
Deionized water	-	Laboratory made (AKR0-C2, Jinan Aiken Technology Co., Ltd.)
Commercial activated carbon		Fujian Xinsen Carbon Co., Ltd.

Table S2. Synthesis parameters of the prepared porous carbon samples.

Sample	Additive dosage (g)	Carbonization temperature (°C)	Carbonization time (h)
AWC-0	0	700	1
AWC-M-0.25	6.7	700	1
AWC-M-0.5	13.4	700	1
AWC-M-0.75	20.1	700	1
AWC-M-1	33.5	700	1
AWC-M-1.25	40.2	700	1
AWC-K-0.25	2.5	700	1
AWC-K-0.5	3.75	700	1
AWC-K-0.75	7.5	700	1
AWC-K-1	10	700	1
AWC-K-1.25	12.5	700	1

Table S3. The I_D/I_G value of AWCs.

Sample	I_D/I_G
AWC-M-0.25	0.8794
AWC-M-0.5	0.9106
AWC-M-0.75	0.9262
AWC-M-1	0.9587
AWC-M-1.25	0.9425
AWC-K-0.25	0.9785
AWC-K-0.5	0.9850
AWC-K-0.75	1.0048
AWC-K-1	1..0578
AWC-K-1.25	1.0354

Table S4 Thomas model fitting parameters for the cyclic breakthrough curves of AWC-M-1 and AWC-K-1.

Samples	k ($L\cdot mg^{-1}\cdot min^{-1}$) × 10^{-4}	q ($mg\cdot g^{-1}$)	R^2
AWC-M-1			
1	11.7	389.6	0.989
2	11.3	380.1	0.991
3	10.6	379.5	0.993
4	10.3	376.1	0.994
5	10.1	377.8	0.993
AWC-K-1			
1	9.83	372.4	0.985
2	9.84	355.6	0.987
3	9.72	332.8	0.990
4	9.69	314.3	0.991
5	9.12	295.3	0.991

Table S5. Textural characteristics of AWC-M-1 (Fresh, Used, Regeneration) and AWC-K-1 (Fresh, Used, Regeneration) samples.

Samples	S_{BET} ($m^2 \cdot g^{-1}$)	V_{Total} [a] ($cm^3 \cdot g^{-1}$)	V_{Micro} [b] ($cm^3 \cdot g^{-1}$)	V_{Meso} [b] ($cm^3 \cdot g^{-1}$)
AWC-M-1 (Fresh)	1209.21	1.5648	0.3342	0.7830
AWC-M-1 (Used)	604.98	0.9757	0.1725	0.4989
AWC-M-1 (Regeneration)	1106.54	1.4542	0.3090	0.6908
AWC-K-1 (Fresh)	1220.29	0.6816	0.4996	0.0990
AWC-K-1 (Used)	983.55	0.4987	0.2997	0.0592
AWC-K-1 (Regeneration)	803.37	0.5112	0.3512	0.0724

a. The single point total pore volume was calculated at $P/P_0 = 0.9989$.

b. V_{Micro} and V_{Meso} were calculated by the NLDFT method.

Table S6. Preparation cost analysis of AWC-M-1.

Program	Unit Cost	Consumption	Expense (USD)
Carbon Source	0	5 kg×4	0
MgO	2.5 USD·kg^{-1}	0.03 kg×4	0.30
N_2	1.63 USD·m^{-3}	0.025 m^3×4	0.16
CH_3COOH*	0.50 USD·kg^{-1}	9.23 kg×4	18.46
Energy consumption of carbonization process	0.05 USD·kWh^{-1}	1 h×2 kW×4	0.40
Energy consumption of evaporation process	0.05 USD·kWh^{-1}	3 h×0.6 kW×4	0.36
Energy consumption of drying process	0.05 USD·kWh^{-1}	1 h×0.6 kW×4	0.12
Labor (operation & maintenance)	0.048 USD·kg^{-1}	5 kg×4	0.96
Depreciation of the apparatus	0.006 USD·Kg^{-1}	5 kg×4	0.12
The costs of logistics to bring the feedstock	0.02 USD·kg^{-1}	5 kg×4	0.40
Summation			21.28
Carbon production (kg)			4.30
Unit Cost (USD·kg^{-1})			4.95

* The price of chemicals is the recent transaction price of bulk chemicals (2/28/2026).